Comparative Analysis of Different Biophysical Techniques for Exosome Characterization

Xiaojuan Yu [1, †], Zhaoxing Wang [2, 3, †], Ruifeng Zhang [2, 3], Wenli Guo [2, 3], Qing Chang [2, 3], Wendan Chu [2, 3], Chengshi Zeng [3], Lan Wang [1, *], Chuanfei Yu [1, *] and Wenqi Li [2, 3, *]

[1] National Institutes for Food and Drug Control, State Key Laboratory of Drug Regulatory Science, NHC Key Laboratory of Research on Quality and Standardization of Biotech Products, NMPA Key Laboratory for Quality Research and Evaluation of Biological Products, Beijing, China.

[2] Core Facility for Biomolecule Preparation and Characterization, Technology Center for Protein Sciences, Tsinghua University, Beijing, China.

[3] Beijing Frontier Research Center for Biological Structure, Tsinghua University, Beijing, China.

* Correspondence: liwenqi@mail.tsinghua.edu.cn (W L); L W; C Y.

[†] These authors contributed equally.

Abstract

Exosomes, as key mediators of intercellular communication, have demonstrated great potential in drug delivery. However, their accurate characterization remains challenging due to their complex physical properties. This study purified exosomes from milk and human urine using ultracentrifugation and the EXODUS systems and systematically compared several biophysical techniques to characterize them, including dynamic light scattering (DLS), nanoparticle tracking analysis (NTA), NanoCoulter technology, and analytical ultracentrifugation (AUC). DLS was found to be suitable for the rapid preliminary assessment of homogeneous samples but it is sensitive to large particles and has limited repeatability. NTA provides better resolution of particle size distribution and dynamic changes. NanoCoulter offers absolute particle concentration but is constrained by its detection range, and AUC demonstrates unique advantages in assessing sample purity using sedimentation behavior and UV absorption. The study findings suggest that a single technique is insufficient for comprehensive exosome characterization. Integrating multiple methods for orthogonal validation may help to establish a more reliable exosome characterization system.

Keywords: Exosomes; Characterization; Nanoparticle tracking analysis; Dynamic light scattering; Analytical ultracentrifugation

1. Introduction

Exosomes, the smallest members (approximately 30–150 nm in diameter) of the extracellular vesicle family, are released into the extracellular environment following the fusion of intracellular multivesicular bodies with the plasma membrane[1–3]. Nearly all cell types can secrete exosomes, which are also naturally present in bodily fluids such as milk, bile, urine, semen, and blood[4,5]. The unique biogenesis of exosomes allows them to carry important biomolecules from their parent cells, including proteins, nucleic acids (e.g., mRNA, miRNA), and lipids, playing a critical role as key messengers in intercellular

communication[6–8].

In recent years, exosomes have garnered significant attention due to their advantages such as small size, good biocompatibility, low toxicity, and low immunogenicity[9,10]. Unlike liposomes or other artificially synthesized nanodrug carriers, exosomes inherit the characteristics of their parent cells and carry components like proteins and nucleic acids. These properties may confer them with targeting capability and immune-activating functions[11]. For example, exosomes can protect cancer immunotherapy drugs from degradation, thereby extending their circulation time and enhancing targeting efficacy[12]. Several exosome-based drug delivery systems for cancer immunotherapy have entered clinical trials[9]. Furthermore, exosomes are amenable to engineering modifications, which can further improve their drug-loading efficiency and tissue-specific targeting ability[13]. Therefore, exosomes demonstrate broad application prospects as a drug delivery vehicle.

Exosome-based drug delivery systems represent a promising tool, yet their reliable identification and characterization face numerous challenges. These challenges primarily stem from the complexity of exosomes in terms of size, morphology, concentration, cellular origin, and molecular composition[14–16]. Furthermore, the choice of characterization techniques can directly influence the measurement of exosome size, with significant discrepancies potentially arising between different methods[17]. Therefore, systematically comparing and studying various exosome characterization approaches is particularly important. The particle characterization methods commonly used in biology are predominantly based on biophysical techniques, including dynamic light scattering (DLS), nanoparticle tracking analysis (NTA), resistive pulse sensing (RPS), and others[15,18,19]. With technological advancements, more methods have been developed and applied to particle characterization, such as asymmetrical-flow field-flow fractionation (AF4)[20]. Recently, a study characterizing lentiviral vectors introduced analytical ultracentrifugation (AUC) and subjected the technique to orthogonal validation alongside methods like NTA[21].

This study characterized exosomes from milk and human urine subjected to different analytical methods including DLS, NTA, RPS-based NanoCoulter, and AUC. Furthermore, the advantages and limitations of each technique in determining exosome size were explored. The findings demonstrated the potential of AUC in assessing exosome purity. Therefore, combining AUC with orthogonal validation from other techniques will help advance the development of exosome characterization methodologies, providing valuable support for exosome purification and the characterization of exosome-based drug carriers.

2. Results

As detailed in Chapter 4, exosomes were purified from milk and urine using ultracentrifugation (UC) and the fully automated EXODUS exosome extraction system (EXODUS, see Section 4.1.3 for introduction). The nomenclature for all of the exosomes subjected to different processing is provided in Chapter 4. The morphology and size of the purified exosomes were examined using transmission electron microscopy (TEM). As shown in Supplementary Materials Figure S1, their size and shape were consistent with the reported 30–150 nm spherical or cup-shaped vesicles[22–25], confirming the successful isolation of exosomes by both purification methods. Furthermore, we systematically characterized the purified exosomes using multiple biophysical techniques, including DLS, NTA, NanoCoulter,

and AUC, to evaluate the respective advantages and limitations of these methods in exosome characterization.

2.1 Dynamic Light Scattering

DLS, a non-invasive characterization technique based on the Brownian motion of nanoparticles in solution, utilizes the random fluctuations in the intensity of scattered light over time when a laser irradiates the sample[26]. The fluctuation rate is analyzed using an autocorrelation function and ultimately calculated based on the Stokes–Einstein equation. This determines the particles' hydrodynamic diameter (i.e., the hydrated particle size) and its distribution. The DLS technique is commonly employed for the preliminary assessment of exosome size distribution due to its speed, non-destructiveness, simple operation, and ability to provide real-time particle size information in the solution state[14,27–29].

We employed DLS to analyze the particle size distribution of exosomes purified from milk and urine using UC and the EXODUS system. Each sample group was tested five times in replicate. The particle size distribution for each component peak, and the average polymer dispersity index (PDI) value was calculated. The PDI is a parameter in DLS that quantifies the uniformity of particle size distribution. For the DLS instrument used in our study, a PDI value of < 0.15 indicates relatively uniform distribution, while a higher value suggests greater dispersity. The DLS results showed that all of the samples (Milk-UC, Milk-AA-UC, Milk-EXODUS, Urine-UC, Urine-EXODUS) exhibited bimodal distribution (Figures 1a–e, Table 1). The smaller peak (Peak 1) corresponded to particles smaller than 30 nm, which might be attributed to the influence of proteins or other impurities. The main peak (Peak 2) displayed a wide distribution range (35–1000 nm), potentially due to the presence of other types of vesicles or large particle impurities introduced during the extraction process. The average PDI value for Peak 2 in all of the samples was higher than 0.15, indicating non-uniform distribution. Further analysis revealed that components with higher PDI values also showed larger standard deviations across the five repeated measurements (e.g., the standard deviation for the PDI value for Peak 2 in Milk-AA-UC was approximately 11), suggesting that DLS has poor repeatability for samples with polydiversity.

Further comparison of milk exosomes processed by different methods (Figure 1f) revealed that samples purified using the EXODUS system exhibited the most uniform size distribution, followed by those treated with acetic acid for casein precipitation. In contrast, samples obtained by direct UC showed the poorest distribution, with a notably broader signal for small particles (Peak 1), suggesting a higher prevalence of impurities, such as proteins and other small particles. We filtered the differently processed milk exosome samples through a 0.22 μm membrane to evaluate and minimize the interference of large particle impurities in DLS measurements. Post-filtration DLS analysis (Figure S2, Table S1) showed that the distribution range of Peak 2 narrowed to 50–250 nm, indicating that DLS can sensitively detect such changes in particle size. These results further confirm that even a small number of large particles in the sample can significantly interfere with DLS measurements due to their stronger light scattering. Therefore, when performing DLS tests, it is essential to minimize interference from large particles and enhance result accuracy by ensuring sample purity and homogeneity.

Table 1. Particle size distribution and average polymer dispersity index (PDI) values of milk and urine exosomes purified by UC and the EXODUS system as determined by DLS

Sample ID	Size distribution (Peak 1)	PDI (Peak 1)	SD (Peak 1)	Size distribution (Peak 2)	PDI (Peak 2)	SD (peak 2)
Milk-UC	7-23 nm	0.2	0.056	50-820 nm	0.42	0.136
Milk-AA-UC	4-8nm	0.16	4.729	50-510nm	0.36	11.481
Milk-EXODUS	4-9nm	0.14	1.6	60-250nm	0.29	2.803
Urine-UC	5-12nm	0.26	2.192	45-400nm	0.36	10.096
Urine-EXODUS	7-14nm	0.12	1.058	35-250nm	0.35	8.27

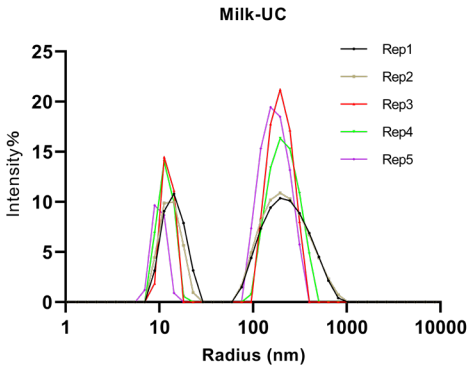

(a)

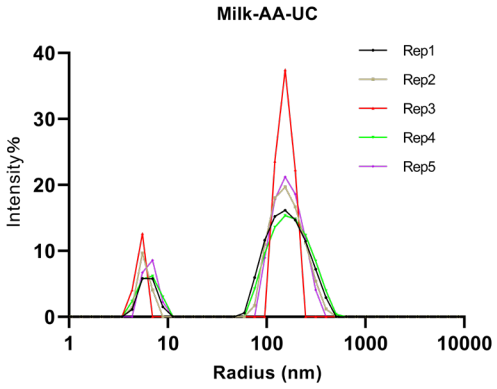

(b)

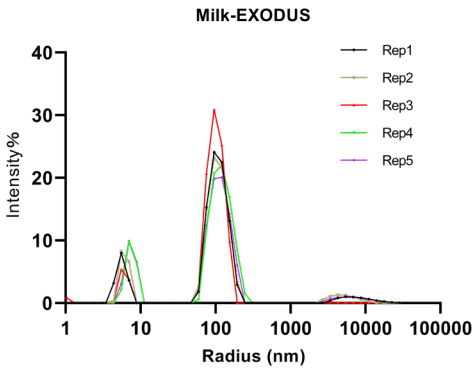

(c)

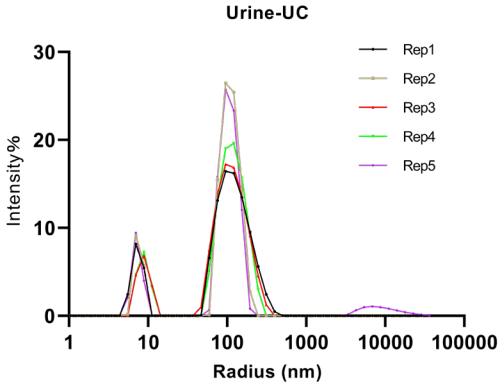

(d)

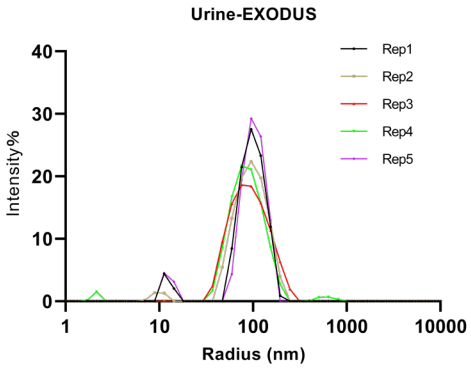

(e)

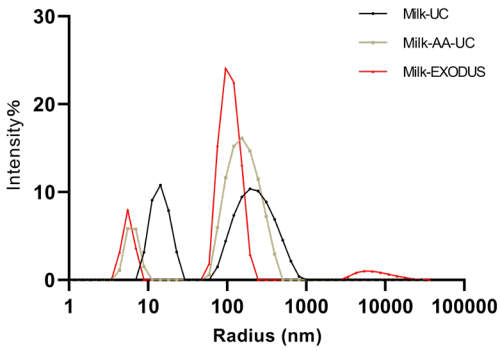

(f)

Figure 1. Dynamic Light Scattering (DLS) results of milk and urine exosomes purified by UC and the EXODUS system: (a) DLS results of Milk-UC, (b) DLS results of Milk-AA-UC, (c) DLS results of Milk-EXODUS, (d) DLS results of Urine-UC, and (e) DLS results of Urine-EXODUS. (f) Comparison of DLS results for exosomes extracted by UC, AA-UC, and the EXODUS system.

2.2 Nanoparticle Tracking Analysis

NTA is a technique that enables the real-time tracking and characterization of individual exosome particles in solution based on the principles of laser light scattering and Brownian motion. By analyzing the Brownian motion trajectory of each particle, NTA can directly calculate its hydrodynamic diameter, thereby providing key physical parameters, including particle size distribution, average particle size, and particle concentration. The single-particle analysis capability of NTA offers higher resolution when assessing complex samples compared to DLS, making it one of the core methods for the physical characterization of exosomes[14,30,31].

Following the same procedure as for DLS testing, we further characterized the exosomes purified from milk and urine by UC and the EXODUS system using NTA. The concentration of all of the samples was pre-evaluated to prevent excessively high sample concentrations from compromising detection accuracy. Each sample was diluted according to the multiples specified in Table 2. The particles in all of the samples (Milk-UC, Milk-AA-UC, Milk-EXODUS, Urine-UC, and Urine-EXODUS) were primarily distributed within the range of 0–400 nm (Figure 2). A comparison of milk exosomes extracted using different methods revealed that samples purified using the EXODUS system exhibited the smallest D50 value and the smallest mean size. In contrast, the UC and AA-UC samples showed relatively larger D50 values, suggesting the presence of more impurities. The particle size distribution plots also visually indicated that milk exosomes purified directly by UC had the broadest distribution and the poorest uniformity. NTA demonstrated higher resolution compared to the DLS results mentioned earlier, allowing for clearer differentiation among the various samples.

To further validate the detection capability of NTA, we conducted comparative experiments involving 0.22 μm membrane filtration and freeze–thaw cycles on selected milk exosome samples (Figure S3). The results showed that the particle size distribution range of the samples filtered through a 0.22 μm membrane became significantly narrower, while samples subjected to freeze–thaw treatment exhibited the noticeable aggregation of large particles. Notably, the average particle sizes measured by NTA in this experiment were generally larger than the typical exosome size range (30–150 nm). This deviation may be attributed to interference from residual impurities in the samples. Products obtained solely

by the UC method tended to contain a relatively higher presence of non-exosome impurities compared to purification techniques such as size-exclusion chromatography or density gradient centrifugation.

Table 2. Particle size distribution of milk and urine exosomes purified by UC and the EXODUS system as determined by NTA

Sample ID	Mean (nm)	D10 (nm)	D50 (nm)	Concentration (particles/mL)	Dilution factor
Milk-UC	208.7	91.2	211.6	$2.91e^{11}$ +/- $5.06e^{10}$	1 x $10e^{3}$
Milk-AA-UC	234.1	157.4	227.2	$4.08e^{11}$ +/- $2.44e^{10}$	1 x $10e^{3}$
Milk-EXODUS	168.8	116.8	156.6	$2.42e^{11}$ +/- $4.01e^{9}$	1 x $10e^{3}$
Urine-UC	177	113.2	161.4	$8.36e^{11}$ +/- $1.11e^{10}$	1 x $10e^{3}$
Urine-EXODUS	156.6	105.9	143.2	$4.76e^{10}$ +/- $2.65e^{9}$	1 x $10e^{2}$

* Mean: Mean particle size; D10: The particle size at the 10th percentile of the cumulative particle size distribution, meaning 10% of the particles are smaller than this size; D50: Median particle size, the particle size at the 50th percentile of the cumulative distribution.

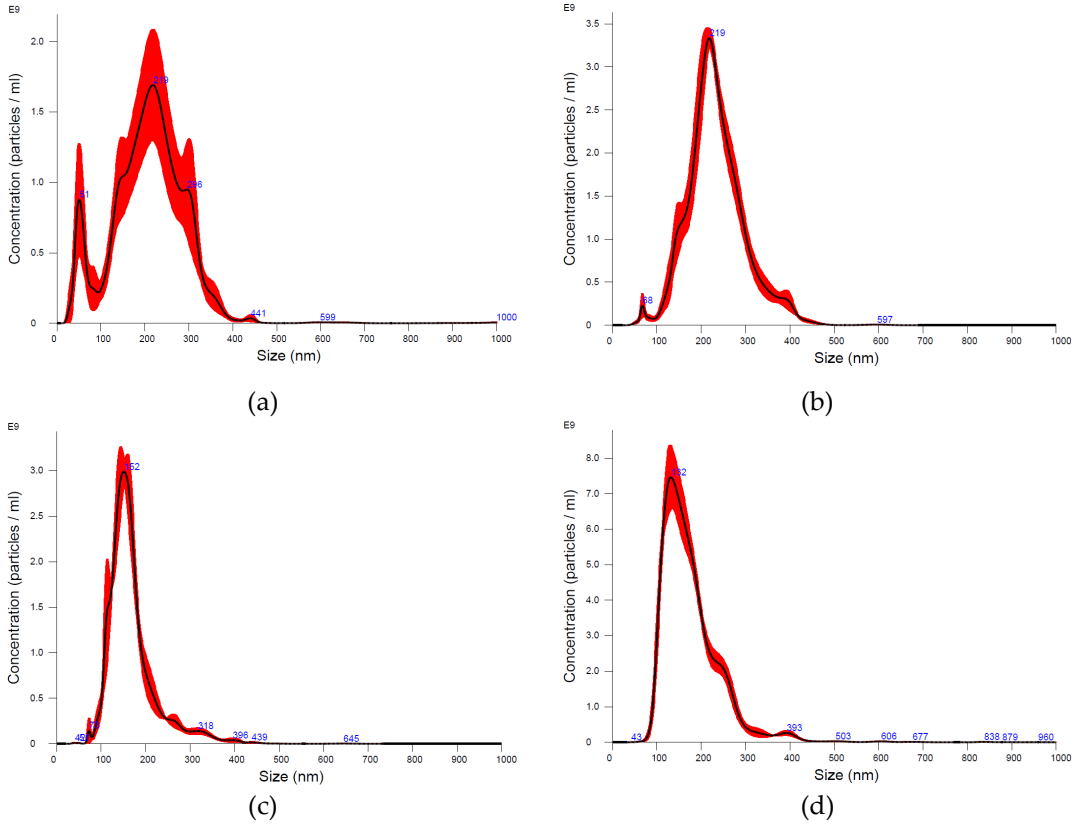

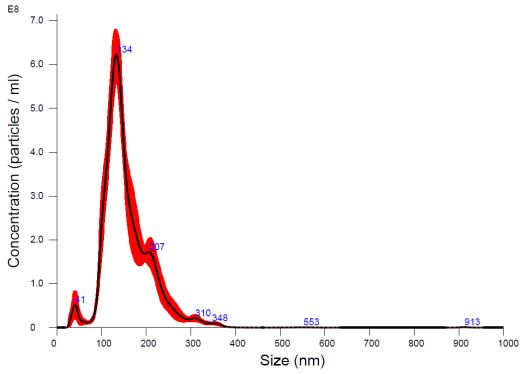

(e)

Figure 2. Nanoparticle Tracking Analysis (NTA) results of milk and urine exosomes purified by UC and the EXODUS system: (a) NTA results of Milk-UC, (b) NTA results of Milk-AA-UC, (c) NTA results of Milk-EXODUS, (d) NTA results of Urine-UC, and (e) NTA results of Urine-EXODUS.

2.3 NanoCoulter technology

NanoCoulter technology is based on the RPS principle, and its core mechanism involves applying a voltage across a chip filled with an electrolyte. When a single exosome particle passes through a nanopore, particle displaces the electrolyte within the pore, causing a transient resistance change, and generating an electrical pulse proportional to the particle's volume. By precisely measuring and analyzing these electrical pulses, this technique can directly and non-optically determine multi-dimensional data for each particle, such as the hydrodynamic diameter, the absolute concentration, and the zeta potential, without relying on any optical models[32,33].

The particle size distribution results obtained using the NanoCoulter method are shown in Figure 3 and Table 3. Regardless of whether the exosomes were extracted by the UC method or the EXODUS system, over 90% of their particle sizes fell within the expected range. Specifically, the mean particle sizes for the Milk-UC, Milk-AA-UC, Milk-EXODUS, Urine-UC, and Urine-EXODUS samples were 92, 95, 88, 78, and 78 nm, respectively. The comparison revealed that the mean particle size of exosomes extracted from urine was significantly smaller than that from milk. Furthermore, the mean particle sizes measured by the NanoCoulter technique were generally smaller than those determined by NTA. This discrepancy is likely because the current detection chip used in the NanoCoulter technique has a lower limit of 50 nm, causing some smaller particulate impurities to be excluded. In contrast, NTA is more susceptible to interference from particulate impurities, often leading to an overestimation of the measured mean particle size.

We conducted comparative filtration and freeze–thaw experiments on milk exosome samples to further evaluate the resolution capability of the NanoCoulter system (Figure S4 and Table S2). Except for the Milk-AA-UC sample, which exhibited a significant decrease in mean particle size after freeze–thaw treatment, the changes in particle size before and after filtration and freeze–thaw cycles were minimal. Unlike the pronounced variations observed with NTA, the differences detected by the NanoCoulter system were relatively small. This may be constrained by the detection limits of the instrument, which could affect its ability to resolve subtle changes in particle size.

Table 3. Particle size distribution of milk and urine exosomes purified by UC and the EXODUS system

as determined by the NanoCoulter technique

Sample ID	Mean (nm)	D10 (nm)	D90 (nm)	Concentration (particles/mL)	Dilution factor
Milk-UC	92	64	132	$3.37e^{11}$	30
Milk-AA-UC	95	63	154	$6.80e^{11}$	50
Milk-EXODUS	88	59	127	$9.68e^{11}$	50
Urine-UC	78	58	117	$6.43e^{11}$	50
Urine-EXODUS	78	55	113	$6.07e^{10}$	50

* Mean: Mean particle size; D10: The particle size at the 10th percentile of the cumulative particle size distribution, meaning 10% of the particles are smaller than this size; D90: The particle size at the 90th percentile of the cumulative particle size distribution.

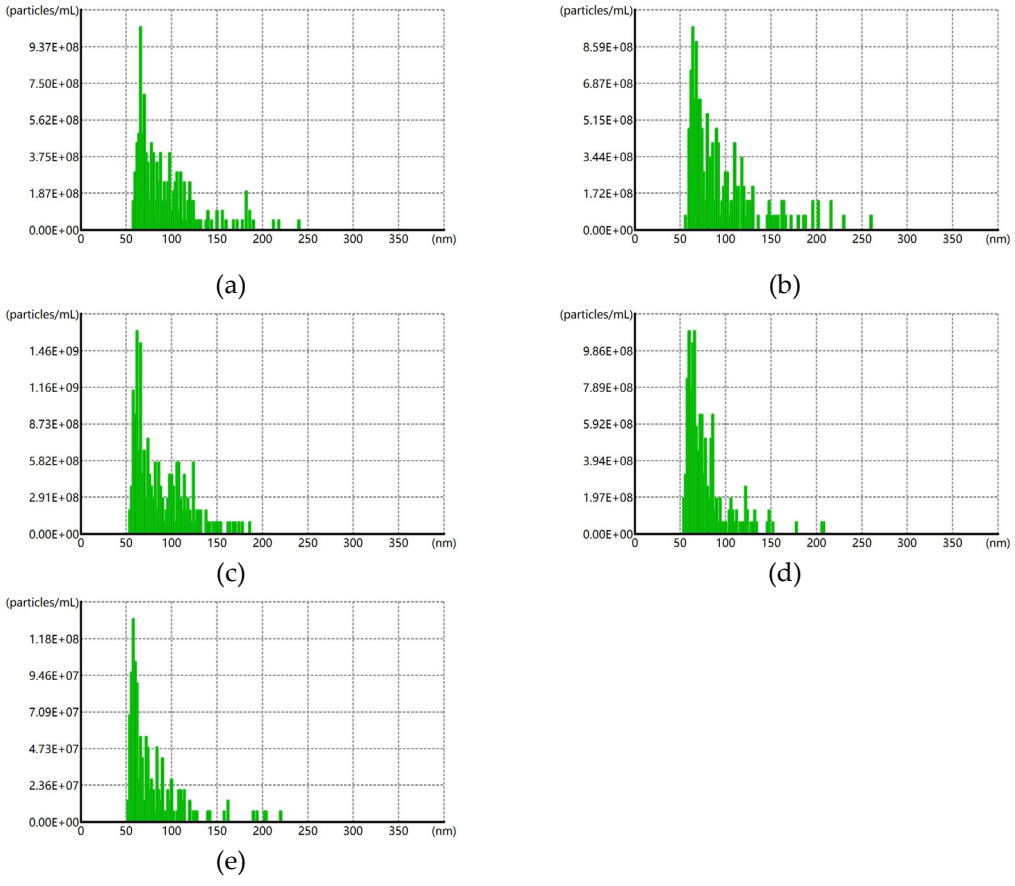

Figure 3. NanoCoulter results of milk and urine exosomes purified by UC and the EXODUS system: (a) NanoCoulter results of Milk-UC, (b) NanoCoulter results of Milk-AA-UC, (c) NanoCoulter results of Milk-EXODUS, (d) NanoCoulter results of Urine-UC, and (e) NanoCoulter results of Urine-EXODUS.

2.4 Analytical Ultracentrifugation

Finally, to systematically evaluate the effectiveness of different purification methods, we characterized the samples using sedimentation velocity-analytical ultracentrifugation

(SV-AUC). This technique, operating in a solution state, monitors the sedimentation process of particles in a powerful centrifugal field in real-time. SV-AUC simultaneously acquires the sedimentation coefficient distribution and UV absorbance characteristics, enabling the label-free analysis of particle size, purity, and homogeneity[34–37].

Milk exosomes subjected to different processing methods were investigated using AUC with absorbance detection at 260 nm (A260) and 280 nm (A280). The AUC results at 7000 rpm revealed that the fitting residual plot of the sedimentation data obtained from Milk-UC (Figures S5 a and b) showed the significant presence of unsettled small particle impurities. In contrast, AA treatment a marked reduction in the corresponding small particle impurities was found (Figures S5 c and d), which aligns with the removal of casein from milk by AA precipitation.

We employed simultaneous dual-wavelength detection at 260 nm (A260) and 280 nm (A280) to analyze the exosomes as comprehensively as possible. Distribution was assessed based on the A260/A280 ratio. As shown in Figures 4a and 4b, where A260/A280 is < 1, these signals are likely attributed to proteins present in the sample, such as casein and whey proteins. This phenomenon was significantly improved after AA precipitation (Figures 4c and 4d). For milk exosomes purified using the EXODUS system, which also removes casein during purification, the fitting residual plot of its sedimentation data (Figures S5 e and f) resembled that of Milk-AA-UC. Considering the sedimentation coefficient distribution in conjunction with the A260/A280 ratio, the primary distribution corresponding to A260/A280 > 1 fell within the 100–500S range. This is because exosomes are mainly composed of lipids, proteins, and various nucleic acids[38]. Since lipids exhibit low UV absorption, studies have confirmed that DNA is the major nucleic acid component of extracellular vesicles, while RNA content is below the detection limit. Therefore, the detected A260/A280 ratio reflects the composition of nucleic acids relative to that of proteins[39,40]. Consequently, AUC can serve as a method to characterize exosomes by distinguishing the sedimentation coefficient distribution of components in exosome samples. However, due to the complexity of exosome particles, AUC currently has limitations in analyzing exosome size distribution. Nevertheless, SV-AUC, which combines sedimentation behavior with absorbance ratios, can effectively differentiate exosomes from co-precipitated protein impurities, providing a unique and powerful tool for evaluating and optimizing exosome purification processes.

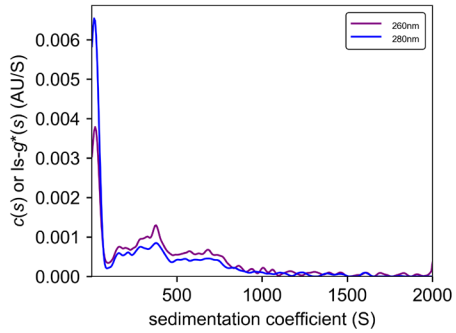

(a)

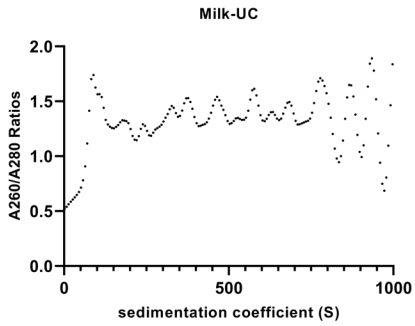

(b)

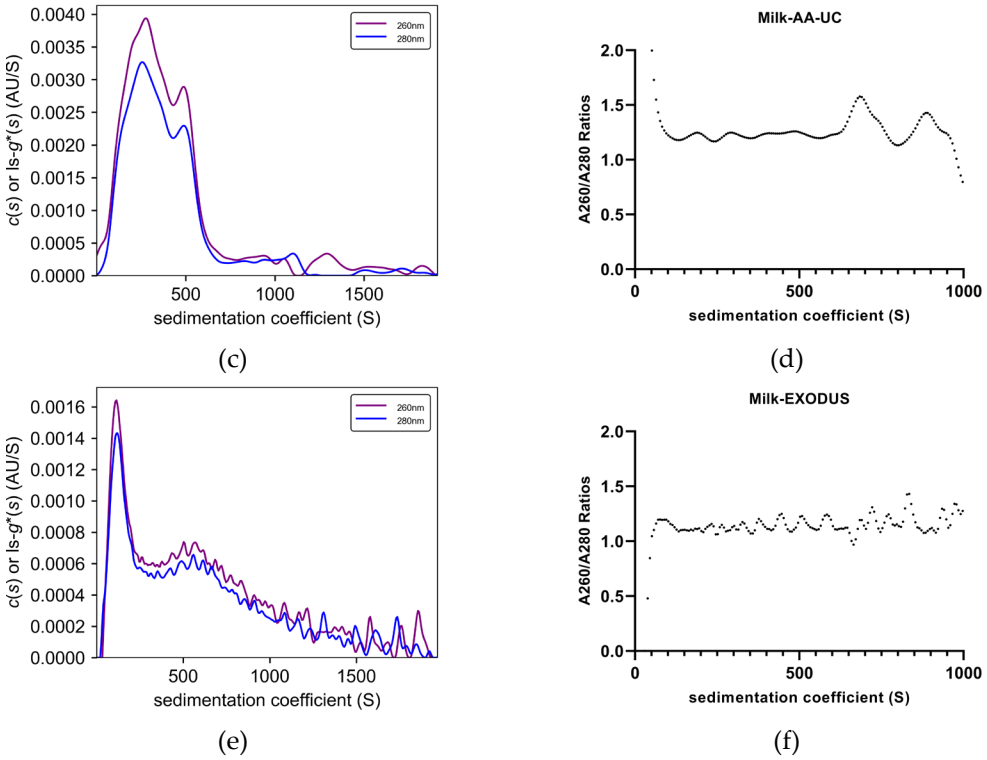

Figure 4. Sedimentation Velocity-Analytical Ultracentrifugation (SV-AUC)analysis of milk exosomes purified by different methods: (a) ls-g*(s) distribution results of Milk-UC, (b) A260/A280 ratio of Milk-UC, (c) ls-g*(s) distribution results of Milk-AA-UC, (d) A260/A280 ratio of Milk-AA-UC, (e) ls-g*(s) distribution results of Milk-EXODUS, and (f) A260/A280 ratio of Milk-EXODUS.

3. Discussion

Exosomes, as key mediators of intercellular communication, require accurate characterization of their physical and biochemical properties for functional studies and applications as drug delivery carriers[41]. However, due to common issues, such as high heterogeneity and co-existing impurities in exosome samples, a single characterization technique often fails to provide comprehensive and reliable information.

In this study, multiple techniques were employed to analyze purified exosomes, clearly revealing the advantages and limitations of each method. For example, while DLS is fast to operate, its analysis of the milk samples in this study revealed excessive sensitivity to trace amounts of large particles and poor repeatability for samples with high polydispersity. This indicates that DLS is more suitable for the preliminary screening of large batches of samples, and yields more accurate results for samples with good homogeneity. NTA, leveraging its single-particle tracking capability, effectively differentiated the particle size distributions of samples obtained by different purification methods and could reveal changes in size distribution under varying processing conditions. NTA currently serves as a core method for characterizing exosome size and concentration. However, NTA is susceptible to interference from the optical properties of impurities, potentially leading to measurement errors. NanoCoulter technology, based on the RPS principle, provides a non-optical measurement of absolute particle concentration, and can accurately measure exosome size distribution. NanoCoulter outperformed both DLS and NTA within the expected size range, showing the

closest agreement with the TEM results. Nonetheless, NanoCoulter limited detection range causes it to overlook smaller particulate impurities, and it does not sufficiently capture particle size changes induced by filtration or freeze–thaw cycles.

SV-AUC demonstrates unique innovative value beyond the aforementioned techniques primarily focused on providing physical size information, serving as a powerful analytical tool. By integrating the sedimentation behavior of particles in a centrifugal field with multi-wavelength UV absorption detection (A260/A280), SV-AUC enables the label-free resolution of sample sedimentation components. When analyzing milk exosomes, SV-AUC could not only differentiate between various components based on their sedimentation coefficient distribution but also clearly distinguished signals originating from protein impurities using the A260/A280 ratio. This provides direct evidence for assessing the effectiveness of purification processes in removing impurities such as proteins. This capability to correlate physical sedimentation characteristics with characteristic optical absorption is not present in other traditional particle size characterization techniques.

4. Materials and Methods

4.1 Exosome Purification

4.1.1 Purification of Milk Exosomes by Ultracentrifugation

For milk samples, initial processing was first performed to remove cellular debris and fat. Fresh milk was centrifuged at 300 ×g for 15 minutes at 4°C. The supernatant was collected and then centrifuged again at 3,000 ×g for 15 minutes at 4°C (this step was repeated once). Subsequently, the supernatant was further clarified by centrifugation at 4°C, 21,500 ×g for 30 minutes.

The pre-treated supernatant described above was subjected to UC at 4°C, 100,000 ×g for 74 minutes, and the supernatant was discarded. To ensure purity, the resulting pellet was resuspended in phosphate-buffered saline (PBS) and centrifuged again under the same conditions (4°C, 100,000 ×g for 74 minutes). The final pellet was resuspended in PBS, and the obtained sample was labeled as Milk-UC.

4.1.2 Purification of Milk Exosomes by Ultracentrifugation in Combination with Acetic Acid Precipitation

After obtaining the supernatant following the 21,500 ×g centrifugation step described in Section 4.1.1, acetic acid was used to adjust the pH to 3.8 to precipitate casein. The mixture was then centrifuged at 4°C, 21,500 ×g for 30 minutes to remove the precipitate. Finally, the supernatant was subjected to UC at 4°C, 100,000 ×g for 74 minutes. The pellet was collected, resuspended in PBS, and the resulting sample was labeled as Milk-AA-UC.

4.1.3 Purification of Milk Exosomes Using the EXODUS Fully Automated Exosome Extraction System

The EXODUS is an automated exosome extraction device (H-600, Shenzhen Huixin Biomedical Technology Co., Ltd., China) that ensures high recovery rates and purity in exosome purification. EXODUS features label-free and automated operation, and is capable of isolating, purifying, and enriching exosomes from samples while removing other impurities. The isolated exosomes maintain high structural integrity and biological activity, making them widely applicable in fields such as proteomics, gene sequencing, metabolomics, in vitro and in vivo functional experiments, drug loading, and therapy. Detailed methods and principles

can be found in the study by Chen et al[8].

First, preliminary centrifugation (4°C, 3,000 ×g for 15 minutes) and filtration were performed to remove fat and debris. Rennet (R920600, Macklin) was then added to the supernatant and incubated in a 37°C water bath for 1 hour to fully coagulate the casein. Whey was obtained by centrifugation at 4°C, 10,000 ×g for 30 minutes. If the whey appeared yellowish, it was treated with proteinase K (S10085, Shanghai Yuanye Bio-Technology Co., Ltd, China) at 37°C for 5 minutes. Subsequently, the sample was diluted 5-fold, filtered through a 0.22 μm membrane, and finally purified using the EXODUS fully automated exosome extraction system. The resulting sample was labeled as Milk-EXODUS.

4.1.4 Purification of Urine Exosomes by Ultracentrifugation

Fresh mid-stream morning urine was centrifuged at 3,000 ×g for 20 minutes at 4°C. The supernatant was then centrifuged at 17,000 ×g for 30 minutes at 4°C. Subsequently, the supernatant was subjected to UC at 200,000 ×g for 2 hours at 4°C. The pellet was collected, resuspended in PBS, and washed by repeating UC under the same conditions (4°C, 200,000 ×g for 2 hours). The final pellet was resuspended in 100 μL of PBS, and the resulting sample was labeled as Urine-UC.

4.1.5 Purification of Urine Exosomes Using EXODUS

Fresh mid-stream morning urine samples were centrifuged at 2000 ×g for 20 minutes at 4°C to remove cellular debris, and the supernatant was collected. The urine supernatant was then filtered through a 0.22 μm filter to eliminate apoptotic bodies and microvesicles. The processed urine samples were transferred to 15 mL or 50 mL centrifuge tubes and finally purified using the EXODUS fully automated exosome extraction system. The resulting sample was labeled as Urine-EXODUS.

4.2 Dynamic Light Scattering

The purified exosome samples (Milk-UC, Milk-AA-UC, Milk-EXODUS, and Urine-UC) were loaded into a detection cuvette. Measurements were conducted using a DLS instrument from Wyatt Technology, with the detection temperature set to 25°C. Each sample was automatically measured 30 times, with each measurement lasting 5 seconds. The correlation function was analyzed using the instrument's accompanying DYNAMICS software. Data were fitted using the cumulant method. The final results are presented as the intensity-weighted average particle size distribution and the polydispersity index value of the sample. Each sample was independently measured in five replicates.

4.3 Transmission Electron Microscopy

All negatively stained samples were prepared using 230-mesh carbon support films (BZ110223b, Beijing Zhongjing Keyi Company). The films were glow-discharged in a vacuum chamber at a current of 30 mA for 20–45 seconds. Subsequently, 10 μL of the sample was applied onto the carbon support film for 120 seconds, after which excess sample was removed using filter paper. The carbon support film was then rinsed 2–4 times with a 10 μL droplet of water (5 seconds each time). Following this, on a piece of cling film, the film was rinsed once for 90 seconds with a 1% uranyl acetate solution (H02624-AB, EMS). Excess uranyl acetate was blotted away with filter paper, and the carbon support film was allowed to air-dry for 120 seconds. Imaging was performed using a Tecnai Spirit transmission electron microscope

(FEI, USA) operating at an acceleration voltage of 120 kV.

4.4 Nanoparticle Tracking Analysis

NTA was performed using a NanoSight NS300 instrument (Malvern Panalytical, United Kingdom) to measure the particle count and size distribution of exosomes isolated by different methods from various sample types. Each sample was diluted with PBS to appropriate multiples (Table 2) to fall within the optimal detection range. Data acquisition and analysis were conducted using NTA software (version 3.4 Build 3.4.003).

4.5 NanoCoulter

The corresponding exosomes were diluted with PBS to appropriate concentrations (Table 3) for subsequent RPS analysis. The particle size distribution of the exosomes was determined using a NanoCoulter counter (NanoCoulter-G, Resun Technology, Co., Ltd, Shenzhen, China) equipped with nanopore chips (measurement range: 150–500 nm).

4.6 Analytical Ultracentrifugation

SV-AUC experiments were performed using 12 mm centerpieces (Beckman, 392778) and a four-hole An60 Ti rotor. Centrifugation was conducted at 7000 rpm using an Optima AUC analytical ultracentrifuge (Beckman Coulter). Absorbance was detected at 20°C, at wavelengths of 280 and 260 nm. Data were analyzed using SEDFIT17 software[42] with the ls-g(s) model to obtain the ls-g(s) sedimentation coefficient distribution profiles.

5. Conclusions

In this study, exosomes from milk and human urine were prepared using UC and EXODUS purification, and their sizes and sedimentation distributions were systematically characterized using techniques such as DLS, NTA, NanoCoulter, and AUC. Comparative analysis validated the distinctive features of each technique in size resolution. DLS was found to be suitable for the rapid preliminary assessment of samples with good homogeneity. NTA performed better in resolving size distributions and their dynamic changes. The NanoCoulter system, limited by its lower detection limit, was more applicable to systems containing larger particles with fewer small-particle impurities, while AUC demonstrated unique advantages in sedimentation analysis, showing significant potential, particularly in assessing sample purity. The research findings indicated that each technique could provide crucial information required for exosome characterization, yet each has its own limitations. Therefore, it is necessary to integrate multiple techniques to achieve a multidimensional and systematic characterization of the physical properties of exosomes, thereby supporting the establishment of a standardized and reproducible exosome characterization system. As the field continues to develop, cross-validation among various analytical methods will become increasingly important.

References

1. Théry, C.; Witwer, K.W.; Aikawa, E.; Alcaraz, M.J.; Anderson, J.D.; Andriantsitohaina, R.; Antoniou, A.; Arab, T.; Archer, F.; Atkin-Smith, G.K.; et al. Minimal Information for Studies of Extracellular Vesicles 2018 (MISEV2018): A Position Statement of the International Society for Extracellular Vesicles and Update of the MISEV2014 Guidelines. *J of Extracellular Vesicle* **2018**, *7*, 1535750, doi:10.1080/20013078.2018.1535750.
2. Merchant, M.L.; Rood, I.M.; Deegens, J.K.J.; Klein, J.B. Isolation and Characterization of Urinary Extracellular Vesicles: Implications for Biomarker Discovery. *Nat Rev Nephrol* **2017**, *13*, 731–749, doi:10.1038/nrneph.2017.148.
3. Liangsupree, T.; Multia, E.; Riekkola, M.-L. Recent Advances in Modern Extracellular Vesicle Isolation and Separation Techniques. *Journal of Chromatography A* **2026**, *1767*, 466602, doi:10.1016/j.chroma.2025.466602.
4. Kalluri, R.; LeBleu, V.S. The Biology , Function , and Biomedical Applications of Exosomes. *Science* **2020**, *367*, eaau6977, doi:10.1126/science.aau6977.
5. Sullivan, R.; Saez, F.; Girouard, J.; Frenette, G. Role of Exosomes in Sperm Maturation during the Transit along the Male Reproductive Tract. *Blood Cells, Molecules, and Diseases* **2005**, *35*, 1–10, doi:10.1016/j.bcmd.2005.03.005.
6. Melo, S.A.; Luecke, L.B.; Kahlert, C.; Fernandez, A.F.; Gammon, S.T.; Kaye, J.; LeBleu, V.S.; Mittendorf, E.A.; Weitz, J.; Rahbari, N.; et al. Glypican-1 Identifies Cancer Exosomes and Detects Early Pancreatic Cancer. *Nature* **2015**, *523*, 177–182, doi:10.1038/nature14581.
7. Liang, K.; Liu, F.; Fan, J.; Sun, D.; Liu, C.; Lyon, C.J.; Bernard, D.W.; Li, Y.; Yokoi, K.; Katz, M.H.; et al. Nanoplasmonic Quantification of Tumour-Derived Extracellular Vesicles in Plasma Microsamples for Diagnosis and Treatment Monitoring. *Nat Biomed Eng* **2017**, *1*, 0021, doi:10.1038/s41551-016-0021.
8. Chen, Y.; Zhu, Q.; Cheng, L.; Wang, Y.; Li, M.; Yang, Q.; Hu, L.; Lou, D.; Li, J.; Dong, X.; et al. Exosome Detection via the Ultrafast-Isolation System: EXODUS. *Nat Methods* **2021**, *18*, 212–218, doi:10.1038/s41592-020-01034-x.
9. Zhang, H.; Wang, S.; Sun, M.; Cui, Y.; Xing, J.; Teng, L.; Xi, Z.; Yang, Z. Exosomes as Smart Drug Delivery Vehicles for Cancer Immunotherapy. *Front. Immunol.* **2023**, *13*, 1093607, doi:10.3389/fimmu.2022.1093607.
10. Chen, R.; Xu, X.; Qian, Z.; Zhang, C.; Niu, Y.; Wang, Z.; Sun, J.; Zhang, X.; Yu, Y. The Biological Functions and Clinical Applications of Exosomes in Lung Cancer. *Cell. Mol. Life Sci.* **2019**, *76*, 4613–4633, doi:10.1007/s00018-019-03233-y.
11. Hazrati, A.; Soudi, S.; Malekpour, K.; Mahmoudi, M.; Rahimi, A.; Hashemi, S.M.; Varma, R.S. Immune Cells-Derived Exosomes Function as a Double-Edged Sword: Role in Disease Progression and Their Therapeutic Applications. *Biomark Res* **2022**, *10*, 30, doi:10.1186/s40364-022-00374-4.
12. Bell, B.M.; Kirk, I.D.; Hiltbrunner, S.; Gabrielsson, S.; Bultema, J.J. Designer Exosomes as Next-Generation Cancer Immunotherapy. *Nanomedicine: Nanotechnology, Biology and Medicine* **2016**, *12*, 163–169, doi:10.1016/j.nano.2015.09.011.
13. Jo, S.D.; Nam, G.-H.; Kwak, G.; Yang, Y.; Kwon, I.C. Harnessing Designed Nanoparticles: Current Strategies and Future Perspectives in Cancer Immunotherapy.

Nano Today **2017**, *17*, 23–37, doi:10.1016/j.nantod.2017.10.008.

14. Szatanek, R.; Baj-Krzyworzeka, M.; Zimoch, J.; Lekka, M.; Siedlar, M.; Baran, J. The Methods of Choice for Extracellular Vesicles (EVs) Characterization. *IJMS* **2017**, *18*, 1153, doi:10.3390/ijms18061153.
15. Khatun, Z.; Bhat, A.; Sharma, S.; Sharma, A. Elucidating Diversity of Exosomes: Biophysical and Molecular Characterization Methods. *Nanomedicine (Lond.)* **2016**, *11*, 2359–2377, doi:10.2217/nnm-2016-0192.
16. Varga, Z.; Yuana, Y.; Grootemaat, A.E.; Van Der Pol, E.; Gollwitzer, C.; Krumrey, M.; Nieuwland, R. Towards Traceable Size Determination of Extracellular Vesicles. *J of Extracellular Vesicle* **2014**, *3*, 23298, doi:10.3402/jev.v3.23298.
17. Chernyshev, V.S.; Rachamadugu, R.; Tseng, Y.H.; Belnap, D.M.; Jia, Y.; Branch, K.J.; Butterfield, A.E.; Pease, L.F.; Bernard, P.S.; Skliar, M. Size and Shape Characterization of Hydrated and Desiccated Exosomes. *Anal Bioanal Chem* **2015**, *407*, 3285–3301, doi:10.1007/s00216-015-8535-3.
18. Maas, S.L.N.; De Vrij, J.; Broekman, M.L.D. Quantification and Size-Profiling of Extracellular Vesicles Using Tunable Resistive Pulse Sensing. *JoVE* **2014**, 51623, doi:10.3791/51623.
19. Van Der Pol, E.; Hoekstra, A.G.; Sturk, A.; Otto, C.; Van Leeuwen, T.G.; Nieuwland, R. Optical and Non-optical Methods for Detection and Characterization of Microparticles and Exosomes. *Journal of Thrombosis and Haemostasis* **2010**, *8*, 2596–2607, doi:10.1111/j.1538-7836.2010.04074.x.
20. Sitar, S.; Kejžar, A.; Pahovnik, D.; Kogej, K.; Tušek-Žnidarič, M.; Lenassi, M.; Žagar, E. Size Characterization and Quantification of Exosomes by Asymmetrical-Flow Field-Flow Fractionation. *Anal. Chem.* **2015**, *87*, 9225–9233, doi:10.1021/acs.analchem.5b01636.
21. Stadler, D.; Helbig, C.; Wuchner, K.; Frank, J.; Richter, K.; Hawe, A.; Menzen, T. Challenges in the Analysis of Pharmaceutical Lentiviral Vector Products by Orthogonal and Complementary Physical (Nano)Particle Characterization Techniques. *European Journal of Pharmaceutics and Biopharmaceutics* **2024**, *200*, 114340, doi:10.1016/j.ejpb.2024.114340.
22. Li, X.; Wang, W.; Chen, J.; Xie, B.; Luo, S.; Chen, D.; Cai, C.; Li, C.; Li, W. The Potential Role of Exosomal miRNAs and Membrane Proteins in Acute HIV-Infected People. *Front. Immunol.* **2022**, *13*, 939504, doi:10.3389/fimmu.2022.939504.
23. Chen, R.; Xu, X.; Tao, Y.; Qian, Z.; Yu, Y. Exosomes in Hepatocellular Carcinoma: A New Horizon. *Cell Commun Signal* **2019**, *17*, 1, doi:10.1186/s12964-018-0315-1.
24. Roma-Rodrigues, C.; Raposo, L.; Cabral, R.; Paradinha, F.; Baptista, P.; Fernandes, A. Tumor Microenvironment Modulation via Gold Nanoparticles Targeting Malicious Exosomes: Implications for Cancer Diagnostics and Therapy. *IJMS* **2017**, *18*, 162, doi:10.3390/ijms18010162.
25. Li, X.; Li, C.; Zhang, L.; Wu, M.; Cao, K.; Jiang, F.; Chen, D.; Li, N.; Li, W. The Significance of Exosomes in the Development and Treatment of Hepatocellular Carcinoma. *Mol Cancer* **2020**, *19*, 1, doi:10.1186/s12943-019-1085-0.
26. Rezaei, N. Cancer Immunotherapy and Nanobiotechnology: An Interdisciplinary Approach.

27. Tiwari, S.; Kumar, V.; Randhawa, S.; Verma, S.K. Preparation and Characterization of Extracellular Vesicles. *American J Rep Immunol* **2021**, *85*, e13367, doi:10.1111/aji.13367.
28. Palmieri, V.; Lucchetti, D.; Gatto, I.; Maiorana, A.; Marcantoni, M.; Maulucci, G.; Papi, M.; Pola, R.; De Spirito, M.; Sgambato, A. Dynamic Light Scattering for the Characterization and Counting of Extracellular Vesicles: A Powerful Noninvasive Tool. *J Nanopart Res* **2014**, *16*, 2583, doi:10.1007/s11051-014-2583-z.
29. Khan, M.A.; Anand, S.; Deshmukh, S.K.; Singh, S.; Singh, A.P. Determining the Size Distribution and Integrity of Extracellular Vesicles by Dynamic Light Scattering. In *Cancer Biomarkers*; Deep, G., Ed.; Methods in Molecular Biology; Springer US: New York, NY, 2022; Vol. 2413, pp. 165–175 ISBN 978-1-0716-1895-0.
30. Erdbrügger, U.; Lannigan, J. Analytical Challenges of Extracellular Vesicle Detection: A Comparison of Different Techniques. *Cytometry Pt A* **2016**, *89*, 123–134, doi:10.1002/cyto.a.22795.
31. Wu, S.; Zhao, Y.; Zhang, Z.; Zuo, C.; Wu, H.; Liu, Y. The Advances and Applications of Characterization Technique for Exosomes: From Dynamic Light Scattering to Super-Resolution Imaging Technology. *Photonics* **2024**, *11*, 101, doi:10.3390/photonics11020101.
32. DeBlois, R.W.; Bean, C.P. Counting and Sizing of Submicron Particles by the Resistive Pulse Technique. *Review of Scientific Instruments* **1970**, *41*, 909–916, doi:10.1063/1.1684724.
33. Yang, M.; Guo, J.; Fang, L.; Chen, Z.; Liu, Y.; Sun, Z.; Pang, X.; Peng, Y. Quality and Efficiency Assessment of Five Extracellular Vesicle Isolation Methods Using the Resistive Pulse Sensing Strategy. *Anal. Methods* **2024**, *16*, 5536–5544, doi:10.1039/D4AY01158A.
34. Patel, T.R.; Winzor, D.J.; Scott, D.J. Analytical Ultracentrifugation: A Versatile Tool for the Characterisation of Macromolecular Complexes in Solution. *Methods* **2016**, *95*, 55–61, doi:10.1016/j.ymeth.2015.11.006.
35. Laue, T.M.; Stafford Iii, W.F. MODERN APPLICATIONS OF ANALYTICAL ULTRACENTRIFUGATION. *Annu. Rev. Biophys. Biomol. Struct.* **1999**, *28*, 75–100, doi:10.1146/annurev.biophys.28.1.75.
36. Lebowitz, J.; Lewis, M.S.; Schuck, P. Modern Analytical Ultracentrifugation in Protein Science: A Tutorial Review. *Protein Science* **2002**, *11*, 2067–2079, doi:10.1110/ps.0207702.
37. Howlett, G.J.; Minton, A.P.; Rivas, G. Analytical Ultracentrifugation for the Study of Protein Association and Assembly. *Current Opinion in Chemical Biology* **2006**, *10*, 430–436, doi:10.1016/j.cbpa.2006.08.017.
38. Wang, N.; Yuan, S.; Fang, C.; Hu, X.; Zhang, Y.-S.; Zhang, L.-L.; Zeng, X.-T. Nanomaterials-Based Urinary Extracellular Vesicles Isolation and Detection for Non-Invasive Auxiliary Diagnosis of Prostate Cancer. *Front. Med.* **2022**, *8*, 800889, doi:10.3389/fmed.2021.800889.
39. Sun, D.; Zhao, Z.; Spiegel, S.; Liu, Y.; Fan, J.; Amrollahi, P.; Hu, J.; Lyon, C.J.; Wan, M.; Hu, T.Y. Dye-Free Spectrophotometric Measurement of Nucleic Acid-to-Protein Ratio for Cell-Selective Extracellular Vesicle Discrimination. *Biosensors and Bioelectronics* **2021**, *179*, 113058, doi:10.1016/j.bios.2021.113058.

40. Patterson, J.; Mura, C. Rapid Colorimetric Assays to Qualitatively Distinguish RNA and DNA in Biomolecular Samples. *JoVE* **2013**, 50225, doi:10.3791/50225.
41. Xu, G.; Jin, J.; Fu, Z.; Wang, G.; Lei, X.; Xu, J.; Wang, J. Extracellular Vesicle-Based Drug Overview: Research Landscape, Quality Control and Nonclinical Evaluation Strategies. *Sig Transduct Target Ther* **2025**, *10*, 255, doi:10.1038/s41392-025-02312-w.
42. Zhao, H.; Sousa, A.A.; Schuck, P. Flotation Coefficient Distributions of Lipid Nanoparticles by Sedimentation Velocity Analytical Ultracentrifugation. *ACS Nano* **2024**, *18*, 18663–18672, doi:10.1021/acsnano.4c05322.

Supplementary Materials

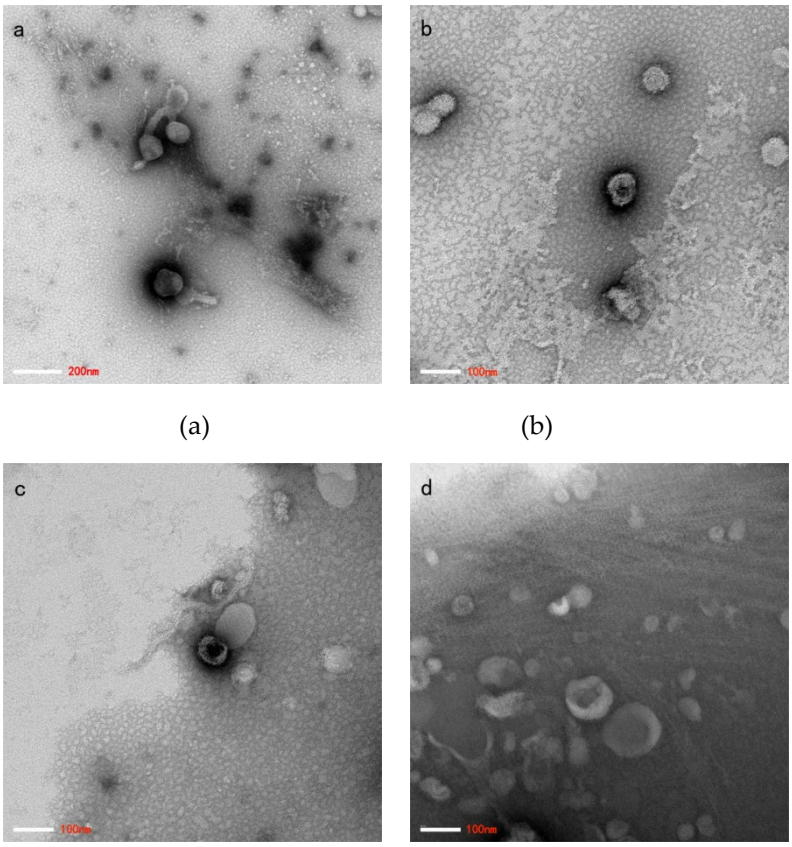

(a) (b)

(c) (d)

Figure S1. Transmission Electron Microscopy (TEM) results of milk and urine exosomes: (a) TEM results of Milk-UC, (b) TEM results of Milk-AA-UC, (c) TEM results of Milk-EXODUS, and (d) TEM results of Urine-UC.

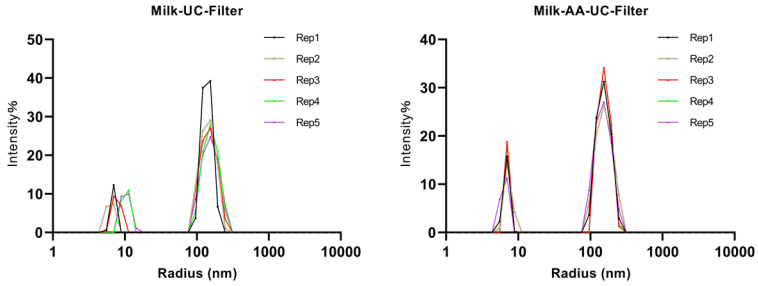

(a) (b)

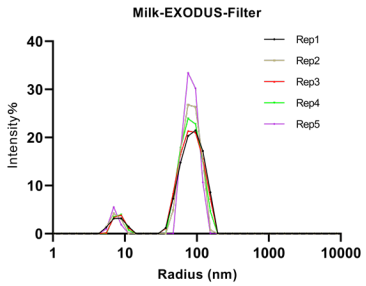

(c)

Figure S2. Dynamic Light Scattering results of filtered milk exosomes: (a) Milk-UC-Filtered results, (b) Milk-AA-Filtered results, and (c) Milk-EXODUS-Filtered results.

Table S1. DLS Results of Particle Size Distribution for Milk Exosomes After Filtration

Sample ID	Size distribution (Peak 1)	PDI (Peak 1)	Size distribution (Peak 2)	PDI (Peak 2)
Milk-UC-Filtered	5-15nm	0.1	50-250nm	0.24
Milk-AA-UC-Filtered	5-10nm	0.08	50-250nm	0.22
Milk-EXODUS-Filtered	5-12nm	0.17	35-200nm	0.3

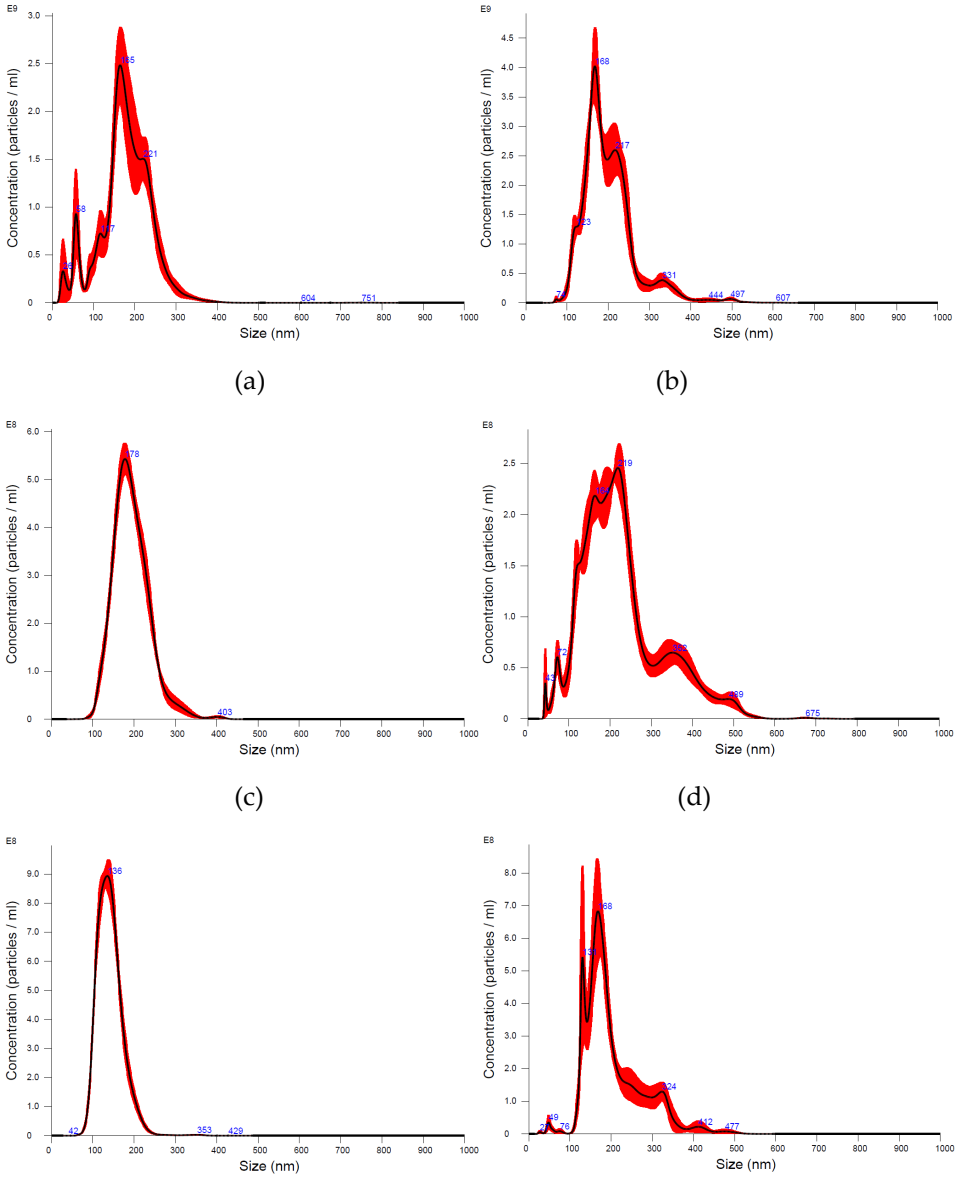

(a) (b)

(c) (d)

(e) (f)

Figure S3. Nanoparticle Tracking Analysis results of filtered and freeze–thawed milk exosomes: (a) Milk-UC-Filtered results, (b) Milk-UC-Freeze–Thaw results, (c) Milk-AA-UC-Filtered results, (d) Milk-AA-UC-Freeze–Thaw results, (e) Milk-EXODUS-Filtered results, and (f) Milk-EXODUS-Freeze–Thaw results.

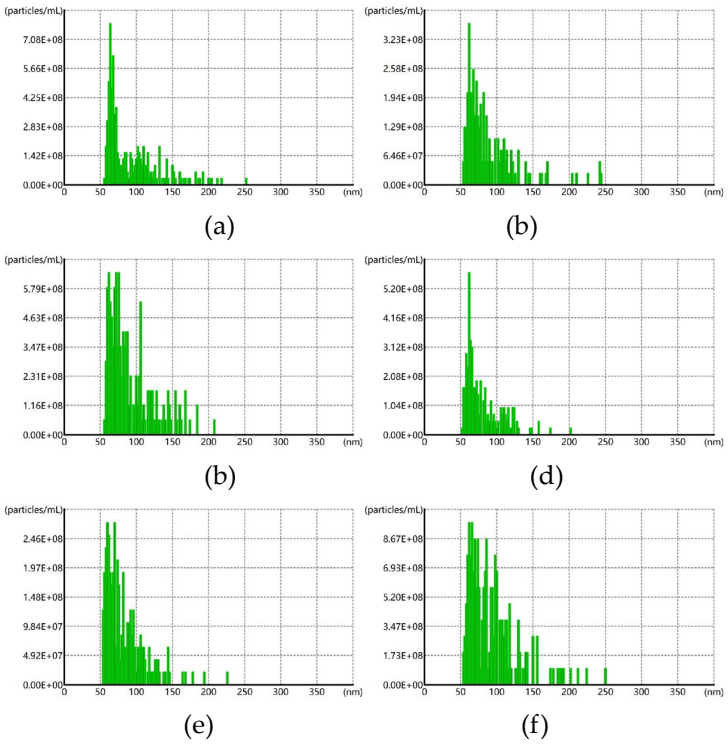

Figure S4. NanoCoulter results of filtered and freeze–thawed milk exosomes: (a) Milk-UC-Filtered results, (b) Milk-UC-Freeze–Thaw results, (c) Milk-AA-UC-Filtered results, (d) Milk-AA-UC-Freeze–Thaw results, (e) Milk-EXODUS-Filtered results, and (f) Milk-EXODUS Freeze–Thaw results.

Table S2. NanoCoulter Results of Particle Size Distribution for Milk Exosomes After Filtration and Freeze–Thaw Treatment

Sample ID	Mean (nm)	D10 (nm)	D90 (nm)	Concentration (particles/ml)	Dilution factor
Milk-UC-Filtered	92	61	149	$3.92e^{11}$	50
Milk-UC-FT	89	60	129	$1.77e^{11}$	40
Milk-AA-UC-Filtered	91	62	139	$5.86e^{11}$	50
Milk-AA-UC-FT	79	57	115	$3.84e^{11}$	80
Milk-EXODUS-Filtered	83	57	120	$2.15e^{11}$	50
Milk-EXODUS-FT	93	61	139	$7.83e^{11}$	40

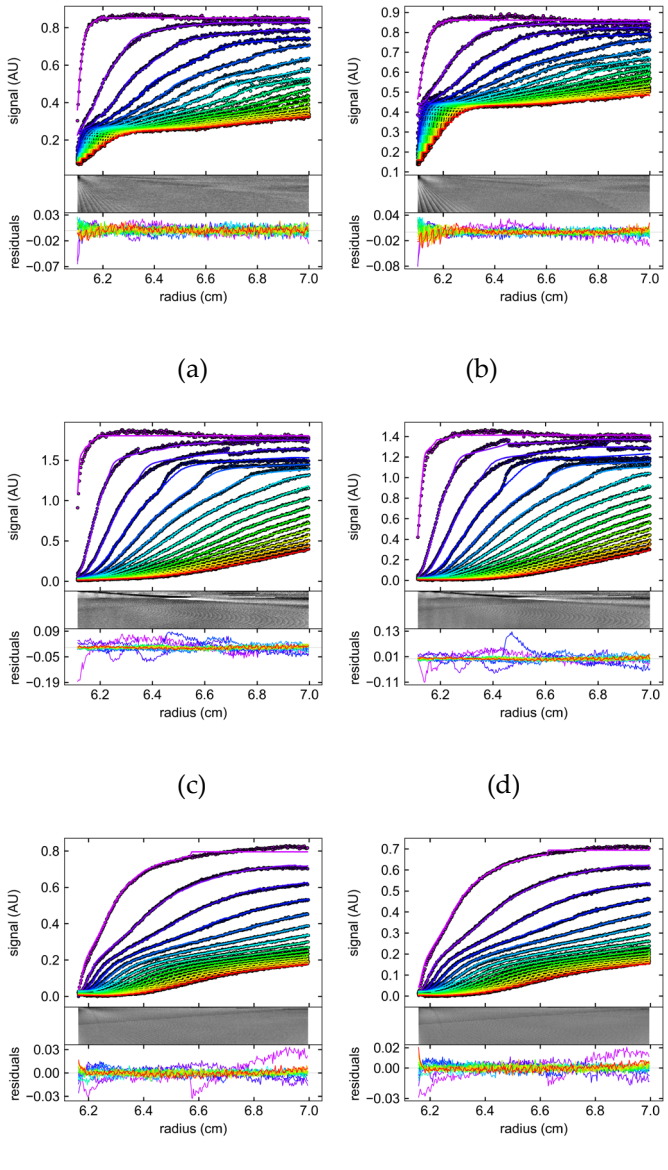

Figure S5. Data fitting residual plots for milk exosomes under different treatments: (a) data fitting residual plot for Milk-UC at 260 nm, (b) data fitting residual plot for Milk-UC at 280 nm, (c) data fitting residual plot for Milk-AA-UC at 260 nm, (d) data fitting residual plot for Milk-AA-UC at 280 nm, (e) data fitting residual plot for Milk-EXODUS at 260 nm, and (f) data fitting residual plot for Milk-EXODUS at 280 nm.